Antibody-drug conjugates targeted to CD79 for the treatment of non-Hodgkin lymphoma

Andrew G. Polson,[1] Shang-Fan Yu,[1] Kristi Elkins,[1] Bing Zheng,[1] Suzanna Clark,[1] Gladys S. Ingle,[2] Dionysos S. Slaga,[1] Lynne Giere,[1] Changchun Du,[1] Christine Tan,[3] Jo-Anne Hongo,[3] Alvin Gogineni,[4] Mary J. Cole,[4] Richard Vandlen,[5] Jean-Philippe Stephan,[6] Judy Young,[6] Wesley Chang,[7] Suzie J. Scales,[2] Sarajane Ross,[1] Dan Eaton,[5] and Allen Ebens[1]

Departments of [1]Translational Oncology, [2]Molecular Biology, [3]Antibody Technology, [4]Tumor Biology and Angiogenesis, [5]Protein Chemistry, [6]Assay Automation Technology, and [7]Pathology, Genentech, South San Francisco, CA

Targeting cytotoxic drugs to cancer cells using antibody–drug conjugates (ADCs), particularly those with stable linkers between the drug and the antibody, could be an effective cancer treatment with low toxicity. However, for stable-linker ADCs to be effective, they must be internalized and degraded, limiting potential targets to surface antigens that are trafficked to lysosomes. CD79a and CD79b comprise the hetrodimeric signaling component of the B-cell receptor, and are attractive targets for the use of ADCs because they are B-cell–specific, expressed in non-Hodgkin lymphomas (NHL), and are trafficked to a lysosomal-like compartment as part of antigen presentation. We show here that the stable-linker ADCs anti-CD79b-MCC-DM1 and anti-CD79b-MC-MMAF are capable of target-dependent killing of non-Hodgkin lymphoma cell lines in vitro. Further, these 2 ADCs are equally effective as low doses in xenograft models of follicular, mantle cell, and Burkitt lymphomas, even though several of these cell lines express relatively low levels of CD79b in vivo. In addition, we demonstrate that anti-CD79b ADCs were more effective than anti-CD79a ADCs and that, as hypothesized, anti-CD79b antibodies downregulated surface B-cell receptor and were trafficked to the lysosomal-like major histocompatibility complex class II–positive compartment MIIC. These results suggest that anti-CD79b-MCC-DM1 and anti-CD79b-MC-MMAF are promising therapeutics for the treatment of NHL. (Blood. 2007;110:616-623)

Introduction

Chemotherapy is at the core of current cancer therapy, and with good reason, because it is effective in many cancers and can be curative in the case of some, such as acute childhood leukemia and Hodgkin disease. However, standard chemotherapy affects normal proliferating tissue, resulting in severe side effects, and therefore is often given at suboptimal doses and risks the health of the patient. Thus, chemotherapy targeted specifically to the cancer cells has the potential to be a highly effective therapy with lower toxicity. This is the goal of developing antibody–drug conjugates (ADCs), in which cytotoxic drugs are attached via chemical linkers to antibodies that recognize cancer cell antigens and thus deliver the cytotoxic drug only to the cells of interest. The linkers within these conjugates are often designed to be cleaved through changes in pH, reduction, or by proteases so that the drug can be preferentially released at the tumor site.[1] Although the idea of ADCs is not novel, developing ADCs as a useful therapeutic faces several daunting challenges in practice[1-4]: (1) the ADC should recognize antigens that are expressed on the surface of cancer cells but not expressed on tissues that are vital or, at a minimum, the antigen-expressing vital cells should not be actively dividing; (2) experience has shown that only very powerful cytotoxic agents are effective as ADCs; however, modest amounts of systemic release of such drugs can result in the toxicities normally associated with traditional chemotherapy; (3) ideally, the drug should be released only when the ADC has entered the cancer cell, which requires designing specialized chemical linkages between the drug and the antibody that are only degraded intracellularly; and (4) even perfectly targeted drugs can cause residual toxicity resulting from the clearance of intact ADC or metabolites.

Non-Hodgkin lymphoma (NHL) is an attractive indication for the development of ADCs as both chemotherapy and antibody therapies have been shown to be individually effective NHL treatments; chimeric IgG1 anti-CD20 (rituximab; Rituxan) in combination with chemotherapy is the standard first-line treatment for the majority of NHLs.[5,6] Rituximab greatly reduces the number of normal as well as malignant B cells and does not result in major side effects, implying that ADC therapeutics for NHL do not need to be completely specific for the tumor but can also target normal B cells without causing serious side effects. While current therapies for NHL have shown some success, treatments for this diverse group of diseases still comprise a major unmet medical need.[7-9]

We have identified CD79, the signaling component of the B-cell receptor (BCR), as a promising ADC target for the treatment of NHL. CD79 has the appropriate expression pattern, being expressed only on B cells and in most NHLs.[10-12] The molecule is a covalent heterodimer containing CD79a (Igα, mb-1) and CD79b (Ig-β, B29); both subunits contain a single extracellular Ig domain, a transmembrane domain, and an intracellular signaling domain. The BCR is a complex between CD79 and surface Ig (sIg), and all of these components are required for surface expression of the

Submitted January 10, 2006; accepted March 5, 2007. Prepublished online as *Blood* First Edition Paper, March 16, 2007; DOI 10.1182/blood-2007-01-066704.

The online version of this article contains a data supplement.

The publication costs of this article were defrayed in part by page charge payment. Therefore, and solely to indicate this fact, this article is hereby marked "advertisement" in accordance with 18 USC section 1734.

BCR.[13] Cross-linking of the BCR triggers its signaling, which can lead to apoptosis or, in the presence of rescue signals from T cells, drive cell activation and cell division.[14] In addition, when the BCR is cross-linked, it is targeted to the major histocompatibility complex class II positive compartment (MIIC), a lysosome-like compartment, as part of class II antigen presentation by B cells.[15] This feature of CD79 biology makes it a particularly attractive target for the use of ADCs as antibodies against CD79 would thus be delivered to these lysosomal compartments. This intracellular CD79 trafficking should allow the use of more stable linkers, which are generally less toxic, because the linker could be cleaved or the antibody degraded in the MIIC, thus releasing the drug only in the targeted cells. In this study, we describe the effective use of such anti-CD79 ADCs with stable linkers in models of NHL.

Materials and methods

Antibodies

Protein for immunization of mice was generated by transient transfection of vectors that express the Fc-tagged or His-tagged extracellular domains of CD79a and CD79b in Chinese hamster ovary cells or 293T cells, and antibodies were generated as previously described.[16] An additional hybridoma for anti-CD79b (SN8)[17] was obtained from Ben Seon (Roswell Park Cancer Institute, Buffalo, NY) and the antibody purified as previously described.[16] Control antibodies, anti-Her2 antibody trastuzumab and anti-HIV gp120, were generated at Genentech. These control antibodies did not bind any of the cell lines used in this study as assayed by flow cytometry.

Anti-CD79b (2F2) was used to generate a mouse-human chimeric antibody. Total RNA was extracted from 2F2 hybridoma cells using a Qiagen RNeasy Mini Kit (Valencia, CA) and the manufacturer's suggested protocol. Using the N-terminal amino acid sequences obtained for the light and heavy chains of the 2F2 monoclonal antibody, polymerase chain reaction primers specific for each chain were designed. Reverse primers for reverse-transcription polymerase chain reaction were designed to match the framework 4 of the gene family corresponding to the N-terminal sequence. The amplified variable light chain was cloned into a pRK mammalian cell expression vector containing the human kappa constant domain (pRK.LPG3.HumanKappa; Genentech, South San Francisco, CA). The amplified variable heavy chain was inserted into a pRK mammalian cell expression vector encoding the full-length human IgG1 constant domain (pRK.LPG4.HumanHC; Genentech) using sites for BsiWI and ApaI. The plasmids were transiently transfected into Chinese hamster ovary cells and the antibody proteins were purified from the transfected cell supernatants on protein A columns; the identity of the purified proteins was confirmed by N-terminal sequencing.

Production of antibody drug conjugates

Maleimidocaproyl–monomethylauristatin F (MC-MMAF) conjugates were produced at Seattle Genetics, Inc (Bothell, WA) according to previously published methods.[18] 4-(N-maleimidomethyl)cyclohexane-1-carboxylate (MCC)-N(2′)-deacetyl-N(2′)-(3-mercapto-1-oxopropyl)-maytansine (DM1) conjugates were prepared as follows. Purified antibody was buffer-exchanged into a solution containing 50 mM potassium phosphate and 2 mM EDTA, pH 7.0. Succinimidyl-4-(N-maleimidomethyl)-cyclohexane-1-carboxylate (SMCC, Pierce, Rockford, IL) was dissolved in dimethyl-acetamide (DMA) and added to the antibody solution to make a final SMCC/Ab molar ratio of 10:1. The reaction was allowed to proceed for 3 hours at room temperature with mixing. The MCC-modified antibody was subsequently purified on a GE Healthcare HiTrap desalting column (G-25) equilibrated in 35 mM sodium citrate with 150 mM NaCl and 2 mM EDTA, pH 6.0. DM1, dissolved in DMA, was added to the MCC-antibody preparation to give a molar ratio of DM1 to antibody of 10:1. The reaction was allowed to proceed for 4 to 20 hours at room temperature with mixing. The DM1-modified antibody solution was diafiltered with 20 volumes of phosphate-buffered saline to remove unreacted DM1, sterile-filtered, and stored at 4°C. Typically, a 40% to 60% yield of antibody was achieved through this process. The preparation was usually greater than 95% monomeric as assessed by gel filtration and laser light scattering. Because DM1 has an absorption maximum at 252 nm, the amount of drug bound to the antibody could be determined by differential absorption measurements at 252 and 280 nm. Typically, the drug to antibody ratio was between 2.5 and 4.5. Although the linker after conjugation is MCC, these ADCs are described in other publications as Antibody-SMCC-DM1,[19,20] we describe them here as MCC-linked ADCs to more accurately reflect the chemical structure.

Xenograft models

All animal studies were performed in compliance with NIH guidelines for the care and use of laboratory animals and approved by the Institutional Animal Care and Use Committee at Genentech. Cells were washed and suspended in Hanks Balanced Salt solution (Hyclone, Logan, UT) and 2×10^7 cells were inoculated subcutaneously into the flank of each female CB17 ICR SCID mouse (6-8 weeks of age; Charles Rivers Laboratories, Hollister, CA) in a volume of 0.2 mL. When mean tumor size reached desired volume, the mice were divided into groups of 8 to 10 mice with the same mean tumor size and dosed intravenously via the tail vein with ADCs or antibodies. In most cases the doses of ADC given to the mice were measured as the mass of the conjugated cytotoxic small molecule drug. For example, mice would be dosed with 100 μg antibody-linked DM1/kg mouse (100 μg/kg), equivalent to 300 μg antibody-linked DM1/m^2 (300 μg/m^2). In some cases the mice were dosed with constant mass of ADC; for example, 5 mg of ADC/ kg mouse. In general, the drug loads on the antibodies in a given experiment were close so these 2 measures were equivalent.

Flow cytometry analysis

For the comparison of CD79b expression on xenograft tumors and normal B cells, recovered tumors were minced and put through a 30-μm cell strainer (BD Biosciences, San Jose, CA) to achieve a single cell suspension. The tumor cells, or peripheral blood, were subsequently prepared by the standard density centrifugation over lymphocyte separation medium (MP Biomedical, Aurora, OH). The resulting single-cell suspension was stained with either a biotinylated isotype control (mouse IgG1) or biotinylated anti-CD79b antibody, followed by streptavidin-APC mixed with anti-CD20-FITC and 7-AAD. The mean fluorescent intensity of CD79b expression was calculated from the CD20-positive 7-AAD–negative population. To follow the expression of the BCR on treated xenograft tumors, a single-cell suspension was prepared as described and then stained with either FITC-conjugated antibody against CD79a or CD22 or IgM, in combination with anti-CD20-APC and 7-AAD. The mean fluorescent intensity of the target expression was calculated from the CD20-positive 7-AAD–negative population.

Bioluminescence imaging

The retroviral construct, pQCXIH.Luc, was generated by cloning the firefly luciferase gene into the pQCXIH retroviral vector (Clontech, Mountain View, CA). Retroviral production and infection were modified from existing protocols.[21,22] Briefly, Phoenix Ampho packaging cells (Orbigen, San Diego, CA) were transfected with pQCXIH.Luc using calcium phosphate. Viral supernatant was collected, supplemented with 10 μg/mL polybrene, and added undiluted to BJAB cells in 6-well plates, which were then centrifuged at room temperature at 300*g* for 45 minutes. Cells were placed into a 32°C incubator for 11 hours to allow viral infection. This procedure was repeated every 12 hours with fresh virus for 2 additional times, followed by the addition of fresh medium and recovery for 48 hours in a 37°C incubator before selection with 400 μg/mL hygromycin for 1 week. The pool of transfected cells was screened for stable luciferase expression for 30 days before use in subsequent experiments.

BJAB-luc cells (5×10^6) were injected into the tail vein of female CB17 ICR SCID mice and the mice were imaged weekly. Before image acquisition, the tumor-bearing mice were anesthetized using isoflurane and injected intraperitoneally with 200 mg/kg D-luciferin (Invitrogen, Carlsbad,

CA). During image acquisition the mice were maintained on isoflurane by nose cone, and body temperature was regulated using a warming pad. Bioluminescence images were acquired using a cooled intensified charge-coupled device camera. Image acquisition times varied according to signal intensity but were typically less than 1 second for the control group, with longer integration times used for the treatment group to rule out the possibility of missing a weak signal. Tumors were localized by overlaying a reference image of the mouse with the bioluminescence data image. Images were quantitated using Image J version 1.37 (developed at the U.S. National Institutes of Health and available online at http://rsb.info.nih.gov/nih-image/) by evaluating pixel intensities in the bioluminescence data image, applying an appropriate background correction and scaling the resulting values to account for variations in acquisition time and camera settings to give a mean intensity in relative light units that was representative of total disease burden. This approach has been validated by pathology and magnetic resonance imaging MRI (data not shown) for other comparable models. Analysis of bioluminescence imaging (BLI) data was performed as follows: Mean relative light units values from each animal image were transformed to the base-10 logarithmic scale for statistical analysis to make the animal-to-animal variability more consistent across groups and time points. For the treatment group, the change in $\log_{10}$ (relative light units) between adjacent time points was analyzed using paired-sample *t* tests. The between-group comparisons did not assume equal variance across groups. The *P* values reported were not adjusted for multiple comparisons.

Immunohistochemistry

BJAB-luc xenograft tumors were collected and immediately placed in optimal cutting temperature (Sakura, Torrance, CA) medium and snap-frozen; 5-μm-thick sections were cut on a cryostat (Leica, Bannockburn, IL), collected on SuperFrost Plus slides (VWR, West Chester, PA), and fixed in acetone for 5 minutes. Sections were blocked for 30 minutes in 10% normal donkey serum, 1% bovine serum albumin in Tris-buffered saline containing 0.05% Tween 20 (Dako, Glostrup, Denmark). Primary antibodies used were fluorescein-conjugated donkey antihuman IgM and Cy3-conjugated goat antimouse IgG (Fcγ-specific; Jackson Immunoresearch, West Grove, PA). Sections were incubated with a mixture of the 2 antibodies for 1 hour, washed with Tris-buffered saline containing 0.05% Tween 20, counterstained with 4′,6-diamidino-2-phenylindole (DAPI; Invitrogen) and coverslipped with ProLong Gold antifade (Invitrogen). Slides were viewed on an Olympus BX-51 microscope equipped with DAPI/FITC/TRITC filter sets and with 20× UPlan Fluor (numerical aperture 0.75) or 100× UPlan Fluor (numerical aperture 1.4) objectives. Images were acquired using a Hamamatsu ORCA charge-coupled device camera driven by MetaMorph software (Molecular Devices, Sunnyvale, CA). Identical camera settings were used for acquisition of images taken in each fluorescence channel to allow comparison of staining intensities between different treatment groups. Individual images were assembled in Adobe Photoshop CS software (Mountain View, CA).

Internalization studies

Ramos cells were incubated for 3 hours at 37°C with 1 μg/mL anti-CD79b: SN8, FcR block (Miltenyi, Auburn, CA) and 25 μg/mL Alexa647-Transferrin (Invitrogen) in complete carbonate-free medium (Invitrogen) and in the presence of 10 μg/mL leupeptin (Roche, Indianapolis, IN) and 5 μM pepstatin (Roche) to inhibit lysosomal degradation. Where indicated, 20 μg/mL brefeldin A (BioMol, Plymouth Meeting, PA) was added during the last 15 minutes of incubation. Cells were then washed twice, fixed with 3% paraformaldehyde (Electron Microscopy Sciences, Hatfield, PA), quenched with 50 mM NH_4Cl (Sigma, St Louis, MO), permeabilized with 0.4% Saponin/2% fetal bovine serum/1% bovine serum albumin, then incubated with 1 μg/mL Cy3 antimouse (Jackson Immunoresearch). After blocking with excess mouse IgG (Invitrogen), cells were incubated with Image-iT FX Signal Enhancer (Invitrogen) followed by Zenon Alexa488-labeled mouse anti-LAMP1 (BD Biosciences) and postfixation with 3% paraformaldehyde. Cells were resuspended in 20 μL buffer and allowed to adhere to poly-lysine (Sigma) coated slides before mounting a coverglass with DAPI-containing VectaShield (Vector Laboratories, Burlingame, CA). Slides were viewed by epifluorescence microscopy with a DeltaVision RT Restoration Imaging System (Applied Precision, Issaquah, WA) equipped with DAPI/FITC/Cy3/Cy5 filters, using a 100× Olympus UplanoApo oil objective (numerical aperture 1.35) and images were captured at room temperature with a Photometrics (Tucson, AZ) CH350 charge-coupled device camera powered by SoftWorx (version 3.4.4; Applied Precision) software. Images were assembled in Adobe Photoshop CS and gamma levels were adjusted for optimal contrast where appropriate.

For immunofluorescence of the MIIC, cells were fixed, permeabilized, and enhanced as above, then costained with zenon-labeled Alexa555-HLA-DM (BD Biosciences) and Alexa488-LAMP1 in the presence of excess mouse IgG per the manufacturer's instructions (Invitrogen).

Results

Anti-CD79b ADCs show target-dependent killing in vitro

We sought to test our hypothesis that CD79 would make a good target for ADCs by testing the effectiveness of 2 different ADC formats whose linkers are stable, such that active metabolite is the cytotoxic drug linked to the conjugating amino acid.[18,19] One format was the maytansinoid DM1 linked to the antibody through the ε-amino group of lysine using the thioester linker MCC.[19] If targeted to the lysosome, MCC-DM1 ADCs can release lysine-Nε-DM1, which is an effective antimitotic agent within the cell. However, once released from the cell, lysine-Nε-DM1 is relatively nontoxic.[19] We also tested the dolastatin-10 derivative MMAF linked to antibody cysteines with a cleavage-resistant MC linker, which on trafficking to the lysosome and degradation releases cysteine-MC-MMAF.[18] Both cytotoxic drugs are mitotic inhibitors that are at least 100-fold more cytotoxic than the vinca alkaloid mitotic inhibitors used in chemotherapeutic treatments of NHLs.[18,19]

We tested the efficacy of these linker drug formats in vitro using the anti-CD79b antibody SN8. All the cell lines tested had a similar sensitivity to free cytotoxic drug (Table 1). The cell lines were less sensitive to free MMAF than to free DM1 because MMAF is relatively membrane impermeable at neutral pH. However, MMAF

Table 1. In vitro sensitivity of lymphoid cell lines to free drug and ADC

	IC50, nM					
	BJAB-luc	SU-DHL-4	DoHH2	Granta-519	Ramos	Jurkat
L-DM1	0.89 (0.08)	1.73 (0.06)	0.15 (0.007)	0.35 (0.01)	0.24 (0.16)	0.49 (0.084)
MMAE	0.53 (0.007)	0.66 (0.006)	0.45 (0.08)	0.36 (0.001)	0.31 (0.02)	0.44 (0.13)
MMAF	60.9 (4.03)	99.4 (3.7)	46.0 (9.16)	43.9 (2.6)	43.22 (6.7)	53.7 (4.31)
anti-CD79 (SN8)-MC-MMAF*	6.84 (0.59)	1.85 (0.08)	1.56 (0.13)	10.38 (0.35)	0.34 (0.02)	>200
anti-CD79 (SN8)-MCC-DM1*	9.65 (0.01)	3.96 (0.30)	10.35 (3.61)	10.51 (0.12)	1.00 (0.14)	63.3 (0.90)

Numbers in parentheses represent standard deviation of quadruplicate assays.
*Concentration of ADC given as the concentration of the conjugated cytotoxic.

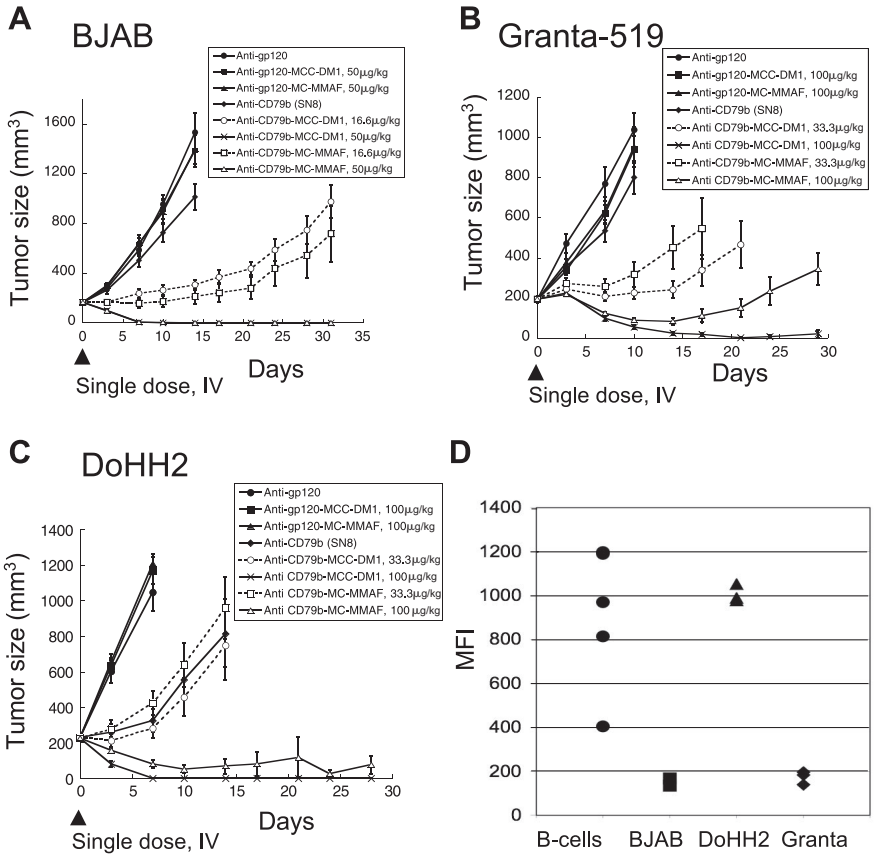

Figure 1. Anti-CD79b ADCs with stable linkers regress tumors in multiple xenograft models. (A) The xenograft tumors of BJAB cells were allowed to grow to an average of 200 mm^3 and then given a single dose intravenously of 50 μg or 16.6 μg of antibody-linked DM1 or MMAF/kg mouse. Unconjugated antibodies were dosed at 3.4 mg antibody/kg, equivalent to the highest amount of conjugated antibody. (B) Granta519 or (C) DoHH2 cell lines were treated as in panel A except that the drug doses were 100 μg or 33.3 μg conjugated DM1 or MMAF/kg mouse and the unconjugated antibody was dosed at 6.8 mg antibody/kg mouse. (D) The levels of surface CD79b expression on dissociated xenograft tumor cells and normal B cells as assayed by flow cytometry.

is extremely potent once inside the cell[18] and all of the cell lines were as sensitive to monomethylauristatin E, a very similar drug that is membrane-permeable, as they were to DM1 (Table 1).[23] Anti-CD79b(SN8)-MCC-DM1 and anti-CD79b(SN8)-MC-MMAF effectively killed 5 NHL cell lines (BJAB-luc, SU-DHL-4, DoHH2, Granta-519, and Ramos), which are CD79-positive, with IC50s ranging from 0.34 to 10.5 nM, but not Jurkat cells (a T-cell line) or Raji cells (an NHL cell line), which do not express CD79 (Table 1, data not shown). These data indicate that the killing seen with the anti-CD79b ADC is target-dependent. Higher concentrations of anti-CD79b(SN8)-MCC-DM1 caused some cell killing of the control cells, but the amount of cell killing corresponded to the amount of killing expected from the approximately 1% of free drug in the anti-CD79b(SN8)-MCC-DM1 preparation (Table 1; data not shown). We also tested the unconjugated anti-CD79b and observed no or minimal effect on cell viability up to 5 μg/mL in our in vitro assays (data not shown). Cell killing by the unconjugated anti-CD79b was a possibility because cross-linking of the BCR can cause apoptosis in some cell lines, although previous reports suggest that anti-CD79 antibodies do not elicit the same levels of signaling and apoptosis as anti-Ig antibodies.[24-26]

Anti-CD79 ADCs are effective in multiple xenograft models

To test if the anti-CD79b ADCs had therapeutic potential in vivo, we tested the efficacy of anti-CD79b(SN8)-MCC-DM1 and anti-CD79b(SN8)-MMAF in 3 xenograft models representative of different types of NHL. The cell lines used in the xenografts contained the canonical translocation associated with the type of NHL. The Burkitt lymphoma cell line BJAB contains the t(2;8)(p12;q24) translocation resulting in the overexpression of myc; the mantle cell lymphoma cell line Granta-519 contains the t(11;14)(q13;q32) translocation resulting in the overexpression of cyclin D1 (BCL1); and the follicular lymphoma cell line DoHH2 contains the t(14;18)(q32;q21) translocation resulting in the overexpression of Bcl-2.[27] The BJAB tumors proved the most responsive to the anti-CD79b ADCs (Figure 1A), followed by DoHH2 (Figure 1C), with Granta-519 tumors (Figure 1B) being the least responsive. Remarkably, a single dose of either anti-CD79b-MC-MMAF or anti-CD79b-MCC-DM1 ADCs resulted in tumor regression or complete remission in all of the tumor models. Interestingly, the MC-MMAF and MCC-DM1 ADCs showed similar efficacies regardless of the cell line used, which is unexpected because the linker and drug chemistries are different. The unconjugated antibody had no or minimal effect in our xenograft models with the exception of DoHH2 xenografts where we observed significant but modest activity (Figure 1A-C).

To determine whether the levels of CD79b expression in vivo could explain the differences in response, we excised each type of xenograft tumor from untreated mice and compared expression levels by flow cytometry. BJAB and Granta-519 cells had similar and much lower amounts of surface CD79b than DoHH2 cells, indicating that the difference in response did not correlate with CD79b expression levels (Figure 1D). In addition, the ability of the cell lines to respond to the anti-CD79b ADCs in the xenograft models did not correspond to the in vitro sensitivity of a given cell line to free drug or anti-CD79b ADCs (Figure 1; Table 1).

Anti-CD79b ADCs are more effective than anti-CD79a ADCs in vivo

The results with ADCs of the anti-CD79b antibody clone SN8 validated CD79b as a target for ADCs in the treatment of B-cell

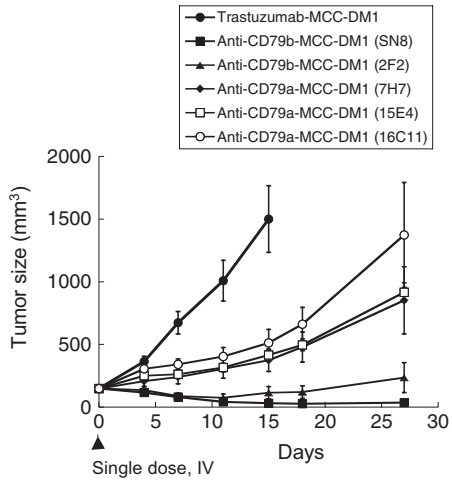

Figure 2. Both anti-CD79a and anti-CD79b ADCs are effective in vivo. BJAB-luc cells (2×10^6) were injected into the flanks of CB17 ICR SCID mice and tumors allowed to grow to an average of 150 mm^3. Groups of 9 mice were treated with a single intravenous dose of 64 μg of antibody-linked drug/kg mouse as indicated.

cancers. We then asked if other anti-CD79 antibodies might be more efficacious. We used Fc or His fusion proteins of the extracellular portion of CD79a and CD79b to generate monoclonal antibodies against these molecules. One anti-CD79b antibody (2F2) and 3 CD79a antibodies (7H7, 15E4, and 16C11) strongly bound surface CD79 on B cells in flow cytometry assays and were selected for further analysis. We tested MCC-DM1 conjugates of these antibodies alongside anti-CD79b (SN8) in the BJAB xenograft model (Figure 2) at a suboptimal dose designed to distinguish the ADCs. Each of the anti-CD79 ADCs was effective in slowing tumor growth, but only the 2 anti-CD79b antibodies (SN8 and 2F2) caused tumor regression. The relative efficacy of the ADCs did not correlate with the affinity of the antibodies as all 3 anti-CD79a antibodies bound cells with higher affinity than anti-CD79b (2F2) as assayed by cell-based enzyme-linked immunosorbent assay (data not shown). These data suggest that CD79b is a better target for ADCs than CD79a, although the reasons for this are unclear. The cell surface copy number is unlikely to be the reason because CD79 is an obligate heterodimer.

Anti-CD79b-MCC-DM1 can completely regress subcutaneous and disseminated xenograft tumors

As a higher bar test for efficacy that would be more representative of human disease, we also examined anti-CD79b-MCC-DM1 treatment in a disseminated tumor model comprising BJAB cells stably expressing luciferase intravenously administered to SCID mice (Figure 3A-C). On day 9 after cell injection, the mice were divided into 2 comparable groups of 8 animals based on established tumor lesions as evaluated by bioluminescence signal and then treated with ADC the next day. The treatment regimen consisted of 2 doses 1 week apart of 5 mg/kg of either control ADC trastuzumab-MCC-DM1 or anti-CD79b(SN8)-MCC-DM1.

After 1 week of treatment (day 16), the average signal in the anti-CD79b-MCC-DM1 group was reduced by approximately 18-fold compared with pretreatment ($P < .001$) with a 125-fold ratio ($P < .001$) between the trastuzumab-MCC-DM1 control group and the anti-CD79b-MCC-DM1 group signals. Signals from all 8 animals in the anti-CD79b-MCC-DM1 group remained suppressed relative to their pretreatment baselines until the final images were taken on day 72, with the exception of one mouse that showed a small tumor burden localized to a lymph node as evaluated by bioluminescence imaging on day 30. The signal increased until the animal was euthanized on day 98 (Figure 3A,3C). The other 7 mice remained healthy until the end of the study on day 152. Mice in the control group had to be euthanized on day 16, day 21 (2 mice), day 23, day 24 (2 mice), day 25, and day 29 because of hind leg paralysis. The difference in survival of the 2 groups (Figure 3A) had a log-ranked P less than .001.

In a separate experiment designed to elicit complete tumor regression, mice bearing BJAB-luc subcutaneous tumors grown to 200 mm^3 before treatment received 3 (as opposed to the single dose used in the previous subcutaneous experiments) weekly doses of 79 μg antibody-linked drug/kg (≈5 mg/kg) anti-CD79b(SN8)-MCC-DM1, which

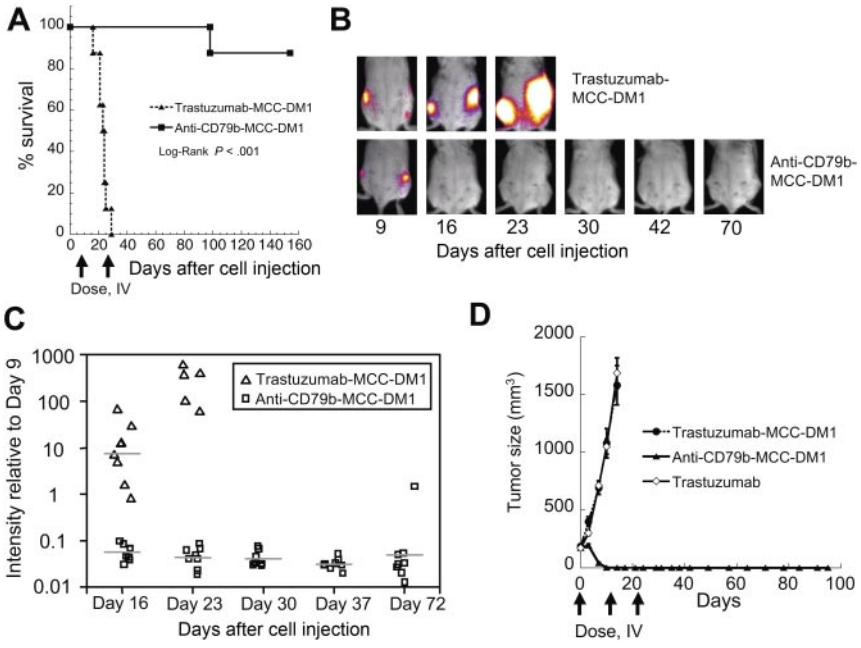

Figure 3. Anti-CD79b-MCC-DM1 can completely regress subcutaneous and disseminated xenograft tumors. Anti-CD79b-MCC-DM1 causes tumor regression in a disseminated tumor model of NHL. Mice were injected intravenously via tail vein with 5×10^6 BJAB-luc cells and grouped into 2 even groups based on tumor burden as evaluated by BLI 9 days after cell injection and treated 2 times 1 week apart with 5 mg ADC/kg mouse (99 μg conjugated DM1/kg mouse) anti-CD79b(SN8)-MCC-DM1 or 5 mg ADC/kg mouse (108 μg conjugated DM1/kg mouse) trastuzumab-MCC-DM1. Tumor burden was evaluated by weekly BLI and mice were euthanized if they became moribund. (A) Kaplan-Meier survival plot of the treated mice. (B) Representative bioluminescence images showing disease progression in a trastuzumab-MCC-DM1 and an anti-CD79b-MCC-DM1 treated mouse. (C) Quantitation of mean bioluminescence intensity for individual animals over time for treatment and control groups. The plot shows variation in signal normalized to the signal intensity just before the start of treatment (day 9). (D) Anti-CD79b-MCC-DM1 can be curative in xenograft models. Growth curves for subcutaneously implanted BJAB cells. Cells were allowed to grow to an average of 200 mm^3 and then given 3 weekly doses intravenous of 79 μg antibody linked drug/kg (≈5 mg/kg) anti-CD79b(SN8)-MCC-DM1 or trastuzumab-MCC-DM1, or 10 mg/kg trastuzumab.

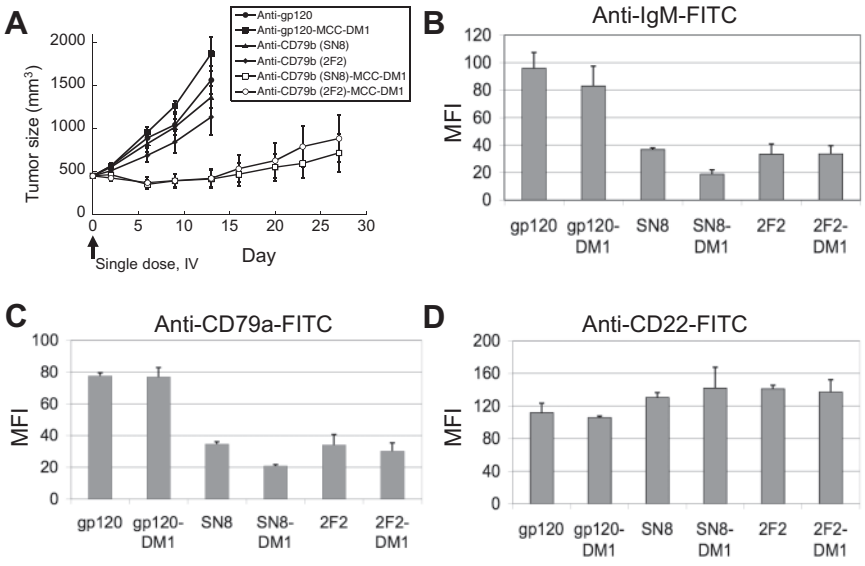

Figure 4. The BCR is downregulated in xenograft tumors treated with anti-CD79b ADCs. The xenograft tumors of BJAB-luc cells were allowed to grow to an average of 450 mm^3 and then given a single dose intravenous ADC equivalent to 66.6 μg of conjugated DM1/kg mouse or unconjugated antibody at 4.5 mg antibody/kg, equivalent to the highest amount of conjugated antibody. After 48 hours tumors from 2 mice in each group were removed and analyzed by flow cytometry for surface IgM, CD79a, and CD22. (A) Plot of tumor volumes for the treated mice. Plot of the average mean fluorescence intensity of the tumors from each group for (B) IgM, (C) CD79a, and (D) CD22.

completely eliminated these tumors as evaluated by caliper measurement. Mice were monitored for 80 days after the final treatment dose and the tumors did not recur and all 10 mice remained healthy (Figure 3D). Control mice treated with trastuzumab-MCC-DM1 were euthanized 14 days after the first treatment because of an excessive tumor burden.

Anti-CD79b is internalized and specifically targeted to the lysosome-like compartment MIIC

We hypothesized that anti-CD79b ADCs cross-link the BCR, causing the internalization of the BCR and delivery of the BCR–ADC complex to the lysosome-like MIIC compartment, where the ADC would be degraded, releasing the cytotoxic drug and/or active metabolite(s) thereof. To test this idea, we asked if the BCR was downregulated on the surface of tumor cells treated with anti-CD79b antibodies or ADCs. Subcutaneous BJAB tumors were allowed to grow to 450 mm^3 and treated with anti-CD79b, anti-CD79b ADCs, control antibodies, or control ADCs (Figure 4A). Two days after drug treatment, tumors were excised from 2 of the mice in each group and the surface expression of the BCR was examined by flow cytometry. Surface expression of CD79a and sIgM were substantially lower in the tumors treated with anti-CD79b antibodies or anti-CD79b ADC compared with tumors treated with control antibodies or ADCs. In contrast, the expression of CD22, another cell surface marker, remained the same regardless of the treatment (Figure 4B-D). Interestingly, the flow cytometry analyses of the anti-CD79b antibody and ADC-treated tumors stained for CD79a or IgM showed a single population, suggesting that all the cells in the tumor were exposed to the antibody or ADC, respectively (data not shown). Immunostaining of portions of these same control (anti-gp120) ADC and the anti-CD79b ADC-treated tumors for mouse IgG (to detect ADC) and IgM (to detect the BCR) also showed that the antibody penetrated the entire tumor, although surface IgM was internalized only in the anti-CD79b ADC-treated tumors (Figure 5A-B, Figure S1, available on the *Blood* website; see the Supplemental Figures link at the top of the online article). This is consistent with the flow cytometry data described, showing a homogenous downregulation of the IgM and CD79a on the surface of anti-CD79b ADC-treated tumor cells in vivo.

To examine the trafficking of the anti-CD79b antibodies in more detail, we looked at localization of antibody after uptake in vitro. All the anti-CD79 antibodies were rapidly internalized within 20 minutes in several CD79-positive cell lines, including BJAB, Ramos, and Daudi (data not shown). Uptake was specific because no signal was detected with an isotype control in these cell lines or with anti-CD79b(SN8) in CD79-negative Raji cells (data not shown). To determine where anti-CD79 antibodies were trafficked, we focused on Ramos because these cells have more spatially separated MIIC/lysosomes and recycling endosomes. Labeling of the MIIC compartment with anti-HLA-DM yielded relatively weak staining, which colocalized perfectly with the brighter lysosomal marker anti-LAMP1 (Figure S2A-C), as would be expected from previously published work;[28] thus the latter was used for further analyses. Anti-CD79b(SN8) started to colocalize with LAMP1 after 1-hour uptake and had significantly accumulated in this compartment by 3 hours (Figure 5C), mostly distinct from the recycling marker transferrin (Figure 5D). This distinction was even more obvious after a 15-minute treatment with brefeldin A, which collapses the recycling endosomes, but not SN8 or LAMP1, into a compact perinuclear pattern[29] (Figure 5E,5F). Thus, anti-CD79b (SN8) is rapidly and efficiently targeted to the MIIC, where it has the potential to be degraded, releasing the active metabolites of the conjugated cytotoxic drugs.

Discussion

The data presented here implicate CD79b as an excellent potential target for ADCs for the treatment of NHL. There are several encouraging aspects to our findings, including the effectiveness of anti-CD79b ADCs at relatively low and infrequent doses. Our data showed that a single dose of anti-CD79b-MC-MMAF or anti-CD79b-MCC-DM1 at just 100 μg/kg (cytotoxic drug) could regress or eliminate xenograft tumors of 3 different types of NHL (Figure 3). In addition, 2 doses of 99 μg conjugated DM1/kg mouse anti-CD79b (SN8)-MCC-DM1 could eliminate disseminated BJAB tumors in 7 of 8 animals treated. Target-independent toxicity studies in rats suggest that

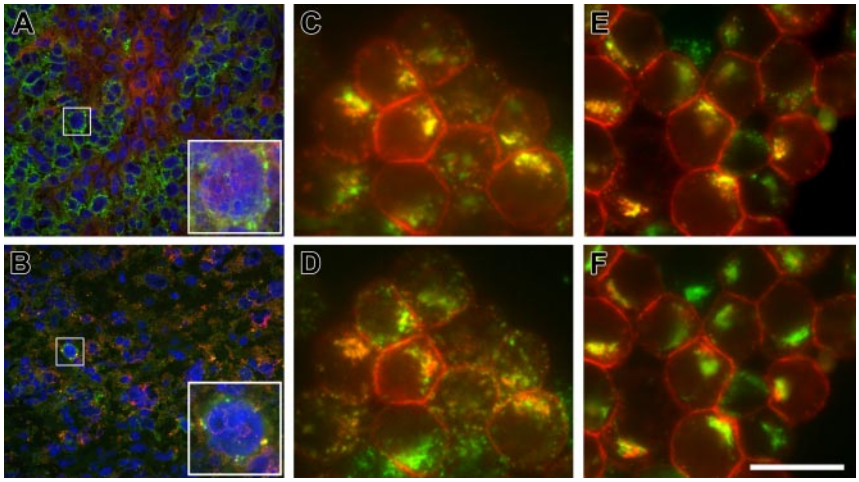

Figure 5. Anti-CD79b antibodies are targeted to the MIIC. Binding and internalization of anti-CD79b antibodies and ADCs in vivo and in vitro. BJAB-luc xenografts were treated with a control mouse anti-gp120-MCC-DM1 conjugate (A) or anti-CD79b(SN8)-MCC-DM1 conjugate (B). Frozen tissue sections were stained with antibodies to human IgM (green) and murine IgG (red); nuclei were counterstained with DAPI (blue). In control-treated xenografts (A), BJAB-luc cells show membrane staining for hIgM; mIgG was clearly detected within the tumor but was not colocalized with hIgM (inset). By contrast, in tumors treated with anti-CD79b(SN8)-MCC-DM1 (B), very few cells were positive for IgM; those that were positive showed colocalization of IgM and the murine IgG in a punctate pattern, consistent with the internalization of the ADC conjugate in these cells (inset). Note the reduced and pyknotic DAPI staining compared with panel A, caused by ADC-mediated cell killing. (C and D) In vitro, Ramos cells were allowed to internalize anti-CD79b(SN8) antibody and Alexa647-transferrin for 3 hours at 37°C in the presence of lysosomal protease inhibitors, then fixed, permeabilized, and stained with Cy3-conjugated anti-mouse antibody. Uptaken anti-CD79b(SN8) (red channel in panels C and D) is efficiently delivered to lysosomes, as shown by its extensive colocalization (yellow color) with the lysosomal marker anti-LAMP1 (Alexa488-labeled, green channel in panel C). There is much less yellow overlap with Alexa647-transferrin (shown in the green channel in panel D for ease of comparison with panel C). (E,F) Cells were labeled as in panels C and D, respectively, except 20 μg/mL brefeldin A was added during the last 15 minutes of uptake to further distinguish recycling endosomes from lysosomes, confirming that uptaken anti-CD79b(SN8) is delivered to lysosomes. The image shown is representative of 7 independent experiments. Scale bar = 20 μm in panels C-E and insets in panels A-B, and 100 μm in main panels A-B.

MC-MMAF antibody conjugates can be dosed up to 90 mg/kg without obvious toxicity,[18] which is particularly encouraging because the doses used in our xenograft efficacy studies in mice corresponds to only 1-6 mg/kg. Assuming that targeting the ADCs to CD79b does not greatly increase the toxicity, these data suggest that anti-CD79b-MC-MMAF and anti-CD79b-MCC-DM1 have the potential for an excellent therapeutic window. Unfortunately, our antibodies do not cross-react with mouse or rat CD79b to enable us to test this directly.

CMC-544 (inotuzumab ozogamicin), which is an anti-CD22 antibody conjugated through an acid-labile linker to N-acetyl gamma calicheamicin dimethyl hydrazide (calichDMH), has shown promising results in Phase 1 clinical trials for the treatment of NHL.[30] The efficacy we observe compares favorably to CMC-544; 3 doses 4 days apart of 160 μg conjugated calichDMH/kg mouse will completely regress a subcutaneous xenograft Burkitt lymphoma model.[31,32] If the stable-linker ADCs fulfill their early promise of greater safety, the results presented here suggest that anti-CD79b-MC-MMAF and anti-CD79b-MCC-DM1, or other stable-linker ADC directed to CD79b, could potentially have an even greater therapeutic window.

The efficacy observed with anti-CD79b ADCs did not correlate with surface expression levels of CD79 (Figure 1), or in vitro sensitivity to free drug or ADCs (Table 1). BJAB and Granta cell xenograft tumors were responsive to the conjugates, despite having surface expression levels of CD79b much lower than found on normal B cells (Figure 1D). Previously published data suggest that the surface expression level of CD79b on follicular lymphoma and diffuse large B-cell lymphoma cells is near or slightly lower than on normal B cells but with a much broader range of expression levels.[11,12] Our data suggest that the surface copy number of CD79b on most NHLs will not be a limiting factor for the efficacy of these ADCs (Figure 1).

Recent publications have suggested that linker-drug combinations such as MC-MMAF and MCC-DM1, which are stable to the point where the active metabolite is the cytotoxic drug linked to the conjugating amino acid, have the potential to be very safe but must be targeted to the lysosome to be effective.[18,19] This observation was part of our rationale for choosing CD79 as a target for ADCs for NHL. Our hypothesis was that anti-CD79b antibodies would be internalized on BCR cross-linking, and be targeted to the MIIC compartment, where the drug could be released. The work described here supports and validates this hypothesis by showing both downregulation of surface BCR on xenograft tumors on exposure to anti-CD79b antibodies or ADCs in vivo, and targeting of the antibodies to the MIIC/lysosome in vitro (Figures 4,5,S1,S2). In addition, we found that ADCs with stable linkers targeted to other equally abundant B-cell-specific targets that are not targeted to the MIIC (eg, CD21, CD20) are not effective in xenograft models of NHL (Polson et al, manuscript in preparation).

An encouraging aspect of the data presented in this study is that DoHH2 cells, which contain the t(14;18)(q32;q21) translocation and, as a result, overexpress the apoptosis inhibitor Bcl2,[33] are also responsive to ADC treatment. The observation that unconjugated anti-CD79b can inhibit tumor growth of DoHH2 cells in vivo (Figure 1C) suggests under some circumstances antibody directed cell cytotoxicity, complement directed cytotoxicity, or apoptosis triggered by CD79 signaling could be contributing to the in vivo efficacy of the ADC. In sum, these data suggest that CD79b ADCs could be effective against follicular lymphoma despite the overexpression of Bcl2 characteristic of these tumors, and that anti-CD79b-ADCs can probably eliminate tumor cells through multiple mechanisms.

CD79 was considered as a target for antibody therapy when it was first discovered.[24,26,34,35] At the time the interest was ignited by the efficacy in treating NHL by targeting the BCR with anti-idiotype antibodies that appeared to affect tumor cells through some combination of triggering apoptosis, antibody directed cell cytotoxicity, and complement directed cytotoxicity. However, the

antibodies have to be made to individual tumors idiotypes, rendering this an impractical therapeutic strategy.[36,37] It was suggested that anti-CD79 antibodies could do the same thing for any potential patient. As shown in this study, unconjugated anti-CD79 antibodies are not effective under most circumstances; however, arming the antibodies with cytotoxic drugs could fulfill the promise of CD79 as a target for antibody therapy.

Acknowledgments

The authors thank Ben Seon (Roswell Park Cancer Institute) for the SN8 hybridoma, Kurt Schroeder for production of anti-CD79 antibodies, Peter Senter (Seattle Genetics, Inc), Damon Meyer (Seattle Genetics, Inc), Mike Elliot, Helga Raab, and Chris Nelson for preparation of drug-conjugated antibodies, Klara Totpal for cell line production, Craig Crowley for helpful advice, Noelyn Kljavin and Kathy Kozak for technical assistance, Becky Yang and Dylan Daniel for the BJAB-luc cell line, Yongmei Chen and Yan Wu for the cloning of 2F2, Lisa Bernstein for biostatistics assistance, and Bill Mallet and Mallika Singh for helpful comments on the manuscript.

Authorship

Contribution: A.G.P. designed research and wrote the paper. M.J.C., R.V., J.S., J.Y., W.C., S.J.S, S.R., D.E., and A.E. designed research. S.Y., K.E., B.Z., S.C., G.I., D.S.S., L.G., C.D., and A.G. performed experiments. C.T. and J.H. provided vital reagents.

Conflict-of-interest disclosure: All the authors are employees of Genentech Inc and declare competing financial interest.

Correspondence: A.G. Polson, Genentech Inc, 1 DNA Way, South San Francisco, CA 94080; e-mail: polson@gene.com.

References

1. Polakis P. Arming antibodies for cancer therapy. Curr Opin Pharmacol. 2005;5:382-387.
2. Garnett MC. Targeted drug conjugates: principles and progress. Adv Drug Deliv Rev. 2001;53:171-216.
3. Lambert JM. Drug-conjugated monoclonal antibodies for the treatment of cancer. Curr Opin Pharmacol. 2005;5:543-549.
4. Wu AM, Senter PD. Arming antibodies: prospects and challenges for immunoconjugates. Nat Biotechnol. 2005;23:1137-1146.
5. Gregory SA, Trumper L. Chemotherapy dose intensity in non-Hodgkin's lymphoma: is dose intensity an emerging paradigm for better outcomes? Ann Oncol. 2005;16:1413-1424.
6. Ghielmini M. Multimodality therapies and optimal schedule of antibodies: rituximab in lymphoma as an example. Hematology Am Soc Hematol Educ Program. 2005;:321-328.
7. Fisher RI, Miller TP, O'Connor OA. Diffuse aggressive lymphoma. Hematology Am Soc Hematol Educ Program. 2004;:221-236.
8. Hennessy BT, Hanrahan EO, Daly PA. Non-Hodgkin lymphoma: an update. Lancet Oncol. 2004;5:341-353.
9. Winter JN, Gascoyne RD, Van Besien K. Low-grade lymphoma. Hematology Am Soc Hematol Educ Program. 2004;:203-220.
10. Cabezudo E, Carrara P, Morilla R, Matutes E. Quantitative analysis of CD79b, CD5 and CD19 in mature B-cell lymphoproliferative disorders. Haematologica. 1999;84:413-418.
11. D'Arena G, Musto P, Cascavilla N, Dell'Olio M, Di Renzo N, Carotenuto M. Quantitative flow cytometry for the differential diagnosis of leukemic B-cell chronic lymphoproliferative disorders. Am J Hematol. 2000;64:275-281.
12. Olejniczak SH, Stewart CC, Donohue K, Czuczman MS. A quantitative exploration of surface antigen expression in common B-cell malignancies using flow cytometry. Immunol Invest. 2006;35:93-114.
13. Matsuuchi L, Gold MR. New views of BCR structure and organization. Curr Opin Immunol. 2001;13:270-277.
14. Niiro H, Clark EA. Regulation of B-cell fate by antigen-receptor signals. Nat Rev Immunol. 2002;2:945-956.
15. Drake JR, Lewis TA, Condon KB, Mitchell RN, Webster P. Involvement of MIIC-like late endosomes in B cell receptor-mediated antigen processing in murine B cells. J Immunol. 1999;162:1150-1155.
16. Polson AG, Zheng B, Elkins K, et al. Expression pattern of the human FcRH/IRTA receptors in normal tissue and in B-chronic lymphocytic leukemia. Int Immunol. 2006;18:1363-1373.
17. Okazaki M, Luo Y, Han T, Yoshida M, Seon BK. Three new monoclonal antibodies that define a unique antigen associated with prolymphocytic leukemia/non-Hodgkin's lymphoma and are effectively internalized after binding to the cell surface antigen. Blood. 1993;81:84-94.
18. Doronina SO, Mendelsohn BA, Bovee TD, et al. Enhanced activity of monomethylauristatin F through monoclonal antibody delivery: effects of linker technology on efficacy and toxicity. Bioconjug Chem. 2006;17:114-124.
19. Erickson HK, Park PU, Widdison WC, et al. Antibody-maytansinoid conjugates are activated in targeted cancer cells by lysosomal degradation and linker-dependent intracellular processing. Cancer Res. 2006;66:4426-4433.
20. Kovtun YV, Audette CA, Ye Y, et al. Antibody-drug conjugates designed to eradicate tumors with homogeneous and heterogeneous expression of the target antigen. Cancer Res. 2006;66:3214-3221.
21. Pear WS, Nolan GP, Scott ML, Baltimore D. Production of high-titer helper-free retroviruses by transient transfection. Proc Natl Acad Sci USA. 1993;90:8392-8396.
22. Baker BW, Boettiger D, Spooncer E, Norton JD. Efficient retroviral-mediated gene transfer into human B lymphoblastoid cells expressing mouse ecotropic viral receptor. Nucleic Acids Res. 1992;20:5234.
23. Doronina SO, Toki BE, Torgov MY, et al. Development of potent monoclonal antibody auristatin conjugates for cancer therapy. Nat Biotechnol. 2003;21:778-784.
24. Nakamura T, Sekar MC, Kubagawa H, Cooper MD. Signal transduction in human B cells initiated via Ig beta ligation. Int Immunol. 1993;5:1309-1315.
25. Kuwahara K, Igarashi H, Kawai T, et al. Induction of tyrosine phosphorylation in human B lineage cells by crosslinking MB-1 molecule of B cell receptor-related heterodimer complex. Biochem Biophys Res Commun. 1993;197:1563-1569.
26. Zhang L, French RR, Chan HT, et al. The development of anti-CD79 monoclonal antibodies for treatment of B-cell neoplastic disease. Ther Immunol. 1995;2:191-202.
27. Drexler HG. The leukemia-lymphoma cell line facts book. San Diego: Academic Press; 2001.
28. Kleijmeer MJ, Morkowski S, Griffith JM, Rudensky AY, Geuze HJ. Major histocompatibility complex class II compartments in human and mouse B lymphoblasts represent conventional endocytic compartments. J Cell Biol. 1997;139:639-649.
29. Lippincott-Schwartz J, Yuan L, Tipper C, Amherdt M, Orci L, Klausner RD. Brefeldin A's effects on endosomes, lysosomes, and the TGN suggest a general mechanism for regulating organelle structure and membrane traffic. Cell. 1991;67:601-616.
30. Fayad L, Verhoef G, Czuczman M, et al. Clinical activity of the immunoconjugate CMC-544 in B-cell malignancies: preliminary report of the expanded maximum tolerated dose (MTD) cohort of a Phase 1 study. American Society of Hematology Annual Meeting. Orlando, FL; 2006.
31. DiJoseph JF, Armellino DC, Boghaert ER, et al. Antibody-targeted chemotherapy with CMC-544: a CD22-targeted immunoconjugate of calicheamicin for the treatment of B-lymphoid malignancies. Blood. 2004;103:1807-1814.
32. DiJoseph JF, Goad ME, Dougher MM, et al. Potent and specific antitumor efficacy of CMC-544, a CD22-targeted immunoconjugate of calicheamicin, against systemically disseminated B-cell lymphoma. Clin Cancer Res. 2004;10:8620-8629.
33. Dyer MJ, Lillington DM, Bastard C, et al. Concurrent activation of MYC and BCL2 in B cell non-Hodgkin lymphoma cell lines by translocation of both oncogenes to the same immunoglobulin heavy chain locus. Leukemia. 1996;10:1198-1208.
34. Vasile S, Coligan JE, Yoshida M, Seon BK. Isolation and chemical characterization of the human B29 and mb-1 proteins of the B cell antigen receptor complex. Mol Immunol. 1994;31:419-427.
35. Nakamura T, Kubagawa H, Cooper MD. Heterogeneity of immunoglobulin-associated molecules on human B cells identified by monoclonal antibodies. Proc Natl Acad Sci USA. 1992;89:8522-8526.
36. Vuist WM, Levy R, Maloney DG. Lymphoma regression induced by monoclonal anti-idiotypic antibodies correlates with their ability to induce Ig signal transduction and is not prevented by tumor expression of high levels of bcl-2 protein. Blood. 1994;83:899-906.
37. Davis TA, Maloney DG, Czerwinski DK, Liles TM, Levy R. Anti-idiotype antibodies can induce long-term complete remissions in non-Hodgkin's lymphoma without eradicating the malignant clone. Blood. 1998;92:1184-1190.